Displays 33 (2012) 173–177

Contents lists available at SciVerse ScienceDirect

Displays

journal homepage: www.elsevier.com/locate/displa

Investigation of Curtain Mura in TFT–TN panels after COG ACF process

Sheng-Ya Wang [a,*], Wei-Hsiang Liao [a], Kei-Hsiung Yang [b]

[a] Institute of Photonic Systems, National Chiao Tung University, Guiren, Tainan, Taiwan
[b] Institute of Imaging and Biomedical Photonics, National Chiao Tung University, Guiren, Tainan, Taiwan

ARTICLE INFO

Article history:
Received 25 October 2011
Received in revised form 21 June 2012
Accepted 7 August 2012
Available online 24 August 2012

Keywords:
Liquid crystal displays
Curtain Mura
LCD optical simulation
Thin film circuit bonding
LCD package

ABSTRACT

We have utilized a transmission ratio (TR) between curtain-shaped (Curtain) Mura and non-Mura zones as a key parameter to characterize the optical appearance of Curtain Mura occurred on a 13.3-in TFT–TN panel (Mura sample) after bonding process to place silicon-based driver-IC chips on one of the panel substrates using anisotropic conductive film as a binder (COG ACF process). Our measured TRs of the Mura sample at zero applied voltage were in good agreement with calculated TRs using optical parameters of the Mura sample derived from the measured Stokes parameters of the liquid crystal (LC) medium in that sample. We conclude that the occurrence of Curtain Mura is dominant by the stress-induced change in the twist angle, less sensitive and insensitive to the corresponding induced changes in the cell gap and pretilt angle of the in-panel-LC medium, respectively. By simulation, we also point out a way to reduce the occurrence of Curtain Mura by designing the cell gap for a 90°-twsit TN panel to satisfy the condition of Gooch–Terry first minimum.

1. Introduction

TFT–LCDs have been widely used in the hand-held mobile and notebook PC displays due to thin, light-weight, and low-power consumption. TFT–LCD modules packaged by chip-on-glass (COG) method using anisotropic conductive film (ACF) as a binder have attracted much attention for thin, light-weight, and slim products. The method of COG ACF [1] process is shown in Fig. 1, where a silicon-based driver-IC chip is bonded to one of the panel substrates by simultaneously applying a high pressure of about 70 MPa and a pulse-heating (pulse-width about 10 s) to the IC chip from the top to about 175 °C to melt the ACF film between the IC chip and the panel substrate. The ACF layer has an original thickness of about 25 μm, and is a thermally melt-able organic material containing uniformly dispersed polymeric balls with a diameter of about 4 μm coated with Au film on their surfaces. The bonding of the IC-chip to the panel is a result of subsequently cooling down to solidify the ACF film after its melting under high temperature and pressure. The heating and cooling of the ACF film to bond IC-chip to the panel substrate generate a residual stress on the panel substrate due to a mismatch in the thermal-expansion coefficients between the panel substrate and the IC chip during the COG ACF process. The occurrences of Curtain Mura (CM) in the proximities of bonded IC chips have been commonly observed after regular COG ACF process and reported to correlate with measured warpage [2] on the panel substrate due to the residual stress. However, the previous publication [2] has only shown a correlation between the occurrences of warpage and CM but has not revealed the mechanism of warpage to cause the optical appearance of CM. In our experiments, we have done similar COG ACF process on both liquid-crystal(LC)-filled and empty TFT–TN panels and observed CM frequently on the LC-filled panels but none on the empty panels. Therefore, we believe that such warpage also occurred on empty TFT–TN panels after COG ACF process because a small thermal capacity of the thin LC layer (about 5 μm in thickness) within the panel was insignificant to alter the thermal-relaxation behavior of the panel (with a total thickness of no less than 600 μm) during the COG ACF process. This was consistent with our observation that, without LC medium in the panel, the warpaged empty panel itself had insufficient optical non-uniformity between crossed polarizers to cause the appearance of CM. Therefore, we believe that the stress-induced panel warpage had to produce an effect on the in-panel LC medium such as changing some of its optical parameters of cell gap, pretilt and twist angles from background values to cause the optical appearance of CM phenomenon.

In this paper, we have defined a transmission ratio (TR) between CM and Normal (non-Mura) zones as an important indicator for the appearance of CM. We have set up experimental schemes to measure TRs directly, and Stokes parameters of the TN medium for points located within CM and Normal zones (shown in Fig. 2) of the 13.3-in TFT–TN panel (Mura sample) at zero voltage. We have calculated TRs using in-panel LC optical parameters derived from measured Stokes parameters on the LC medium and compared them with experimental results obtained from direct measurements of TRs between CM and Normal zones within the Mura

* Corresponding author. Tel.: +886 912001412.
E-mail address: shengyawang@gmail.com (S.-Y. Wang).

0141-9382/$ - see front matter © 2012 Elsevier B.V. All rights reserved.
http://dx.doi.org/10.1016/j.displa.2012.08.002

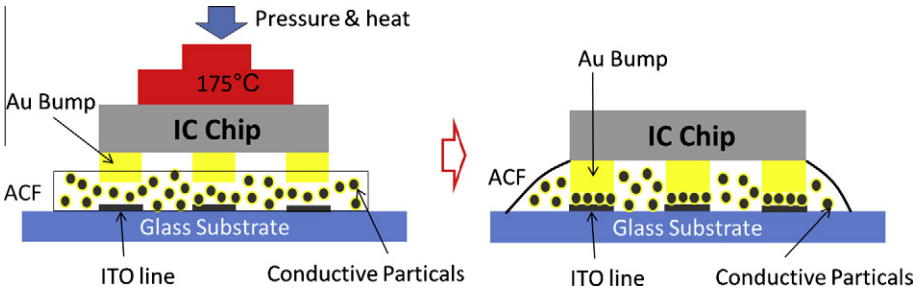

Fig. 1. Schematic illustration of chip-on-glass (COG) process using anisotropic conductive film (ACF) as a binder.

sample at zero voltage. In this paper, in addition to the identification of the key in-panel-LC parameters causing CM, we also suggest a way to reduce the occurrence of CM by designing LC parameters of the TN cell to satisfy the condition of the Gooch–Tarry first minimum in transmission. This paper is organized under the sections of Introduction, Simulation, Experiments on the Measurements of Transmission Ratio, Result and Discussion, Conclusion and Acknowledgements.

2. Simulation

For the purpose of identifying the in-panel LC optical parameters whose deviations from background values might be responsible to cause CM after COG ACF process, we used LCDST V6.0 simulation program [3] to calculate TRs of the Mura sample at normally black mode with optical parameters of cell gap 3.6 μm, twist angle 90°, and pretilt angle 3.8° as standard (or background values) similar to those specified by the panel maker for the Mura sample before COG ACF process. The parameters of the LC medium used in simulations are shown in Table 1. Assuming incident light with wavelength at 589 nm, we have calculated TRs as a function of applied voltage on the Mura sample by changing one of in-panel LC optical parameters such as cell-gap, pretilt and twist angles from standard.

Figs. 3 and 4 showed TR versus R.M.S voltage (TR–*V*) at 1 kHz by changing cell gap and twist angle from standard, respectively. We could see that, below threshold voltage, the TR was sensitive to the deviation of cell gap and twist angle from standard as shown in Fig. 3 and 4, respectively, but almost insensitive to the change in pretilt angle near zero voltage as shown in Fig. 5. These results indicated that the deviations of the twist angle and the cell gap from standard might be responsible for the occurrences of CM after COG ACF process.

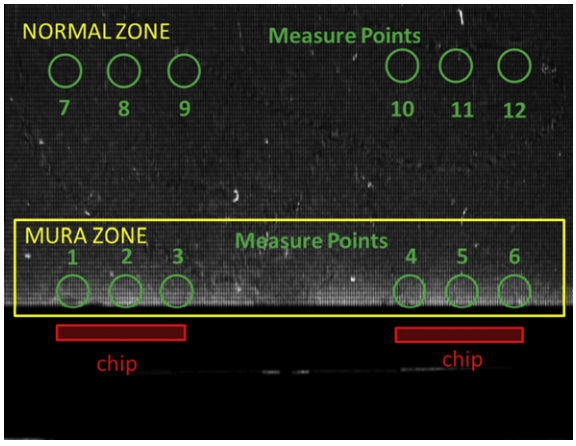

Fig. 2. Curtain Mura and Normal zones on a 13.3-in TFT–TN panel in normally black mode.

3. Experiments on the measurement of transmission ratio

The TR or difference in transmission between CM and Normal zones is the major indicator on the optical appearance of CM

Table 1
Liquid crystal parameters used in simulation.

Refractive index		Dielectric constant		Elastic constant	
n_e	1.597	$\varepsilon_{\parallel}$	11.4	K_{11}	8.6 pN
n_o	1.497	$\varepsilon_{\perp}$	3.6	K_{22}	7.3 pN
				K_{33}	13.7 pN
Wave length λ = 589 nm					

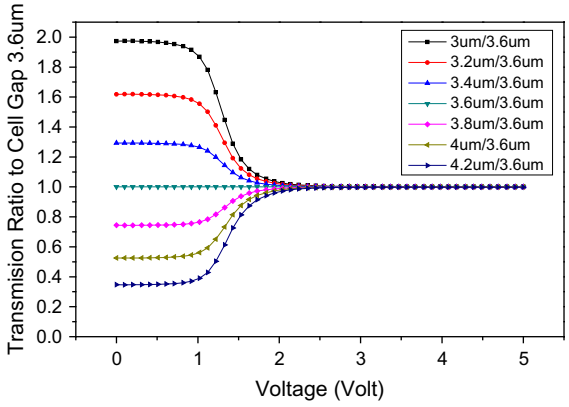

Fig. 3. TR–*V* curves using change in cell gap as a parameter.

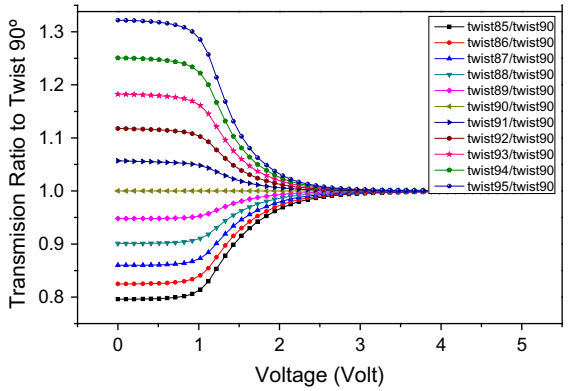

Fig. 4. TR–*V* curves using change in twist angle as a parameter.

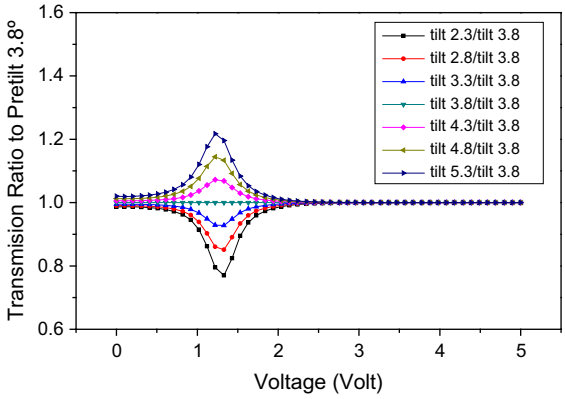

Fig. 5. TR–*V* curves using change in pretilt angle as a parameter.

phenomenon. From the results of simulations, we knew that the variations in twist angle and cell gap might be mainly responsible for the occurrences of CM after COG ACF process. We have set up one experimental scheme (similar to Fig. 7 but without quarter wave plate) to do direct measurements of transmission of the sample by impinging a laser beam through the Mura sample at zero voltage placed between parallel polarizers whose corresponding transmitting axis aligned with respect to the adjacent rubbing direction for LC alignment within the Mura sample, and detected by a photo-diode. Using an incident laser beam passing through a linear polarizer with an extinction ratio of 5000:1 as an incident light source with measured power of 1.3 mW, the measured transmissions (in μw) are shown in Table 2 that indicates a measured TR of 1.13 = 3.046 μw/2.676 μw (the ratio of 6-point-average transmissions between CM and Normal zones, respectively).

3.1. Theoretical background for the experimental measurements of Stokes parameters [4]

In order to calculate TRs on the Mura sample at zero voltage, we have to measure the Stokes parameters for points located within CM and Normal zones of the Mura sample (shown in Fig. 2). We, then, derived optical parameters of the Mura sample at zero voltage from measured Stokes parameters, and used them to calculate TRs of the Mura sample.

For the measurements of Stokes parameters, the coordinate system is shown in Fig. 6. The transmission axis of the entrance polarizer is set parallel to the *y* axis. Entrance LC director forms an angle α with the *x* axis, and TN LC medium is twisted by Φ angle. Jones matrix for the TN LC medium can be represented as:

Table 2
Transmission of each measured points in normally black mode.

Measure points	Transmission (μw)	Average transmission (μw)
CM zone		
1	3.05	3.046 ± 0.035
2	3.06	
3	2.98	
4	3.03	
5	3.09	
6	3.07	
Normal zone		
7	2.64	2.676 ± 0.040
8	2.73	
9	2.66	
10	2.72	
11	2.69	
12	2.62	

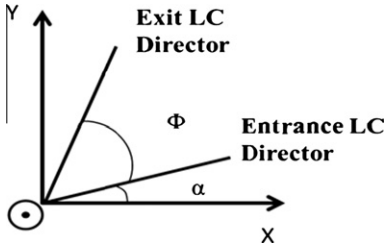

Fig. 6. A coordinate scheme depicts the orientations of the TN cell and incident light beam.

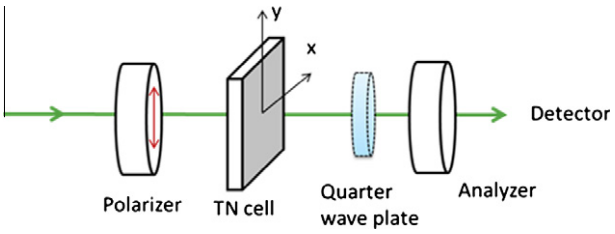

Fig. 7. The experimental scheme for the measurement of stokes parameters.

$$\begin{bmatrix} E_x \\ E_y \end{bmatrix} = \begin{bmatrix} \cos\alpha & -\sin\alpha \\ \sin\alpha & \cos\alpha \end{bmatrix} \begin{bmatrix} a & b \\ -b^* & a^* \end{bmatrix} \begin{bmatrix} \cos\alpha & \sin\alpha \\ -\sin\alpha & \cos\alpha \end{bmatrix} \begin{bmatrix} 0 \\ 1 \end{bmatrix} \tag{1}$$

where a, b, $-b^*$, a^* are the Jones matrix elements of the TN LC medium which can be expressed as [5]:

$$\begin{aligned} a &= a_1 + ja_2 \\ b &= b_1 + jb_2 \end{aligned} \tag{2}$$

Then, a_1, a_2, b_1, b_2 are

$$\begin{aligned} a_1 &= \frac{1}{x}\sin\Phi\sin(x\Phi) + \cos\Phi\cos(x\Phi) \\ a_2 &= \frac{u}{x}\cos\Phi\sin(x\Phi) \\ b_1 &= \frac{1}{x}\cos\Phi\sin(x\Phi) - \sin\Phi\cos(x\Phi) \\ b_2 &= \frac{u}{x}\sin\Phi\sin(x\Phi) \end{aligned} \tag{3}$$

where

$$\begin{aligned} u &= \frac{\pi d}{\lambda\Phi}(n_{\text{eff}} - n_o) \\ x &= \sqrt{1+u^2} \\ n_{eff} &= \frac{n_o n_e}{\sqrt{n_e^2\cos^2\theta + n_o^2\sin^2\theta}} \end{aligned} \tag{4}$$

From Eqs. (1)–(4), we obtain E_x, E_y as:

$$\begin{aligned} E_x &= b_1 + j(a_2 sin2\alpha + b_2 cos2\alpha) \\ E_y &= a_1 + j(-a_2 cos2\alpha + b_2 sin2\alpha) \end{aligned} \tag{5}$$

Using Eq. (5), we deduce the Stokes parameters of transmitted light through the TN medium as expressed in the following equation:

$$\begin{aligned} S_0 &= E_x E_x^* + E_y E_y^* = a_1^2 + a_2^2 + b_1^2 + b_2^2 = 1 \\ S_1 &= E_x E_x^* - E_y E_y^* = b_1^2 - a_1^2 - a_2^2 cos4\alpha + b_2^2 cos4\alpha + 2a_2 b_2 sin4\alpha \\ S_2 &= E_x E_y^* + E_x E_y^* = 2a_1 b_1 + (b_2^2 - a_2^2) sin4\alpha - 2a_2 b_2 cos4\alpha \\ S_3 &= j(E_x E_y^* - E_x E_y^*) = 2b_1(b_2 sin2\alpha - a_2 cos2\alpha) \\ &\quad - 2a_1(a_2 sin2\alpha + b_2 cos2\alpha) \end{aligned} \tag{6}$$

Table 3
Stokes parameters of each measure points.

Measure points	Stokes parameters		
	S_1	S_2	S_3
CM Zone			
1	0.754	−0.432	0.495
2	0.751	−0.452	0.481
3	0.772	−0.413	0.484
4	0.769	−0.418	0.484
5	0.752	−0.456	0.476
6	0.772	−0.426	0.472
Normal zone			
7	0.775	−0.394	0.494
8	0.772	−0.403	0.491
9	0.796	−0.384	0.469
10	0.808	−0.371	0.457
11	0.782	−0.385	0.490
12	0.795	−0.363	0.487

Table 4
Derived twist angles and cell gaps of each measured points.

Measure points	Cell gap (μm)	Twist angle (°)	Average cell gap/twist angle
CM zone			
1	3.551	93.054	Cell gap: 3.56 ± 0.012 μm,
2	3.552	94.001	
3	3.578	92.716	
4	3.574	92.871	Twist angle:
5	3.554	94.24	93.379 ± 0.567°
6	3.580	93.392	
Normal zone			
7	3.580	91.901	Cell gap: 3.60 ± 0.019 μm,
8	3.577	92.247	
9	3.612	92.174	
10	3.632	92.053	Twist angle: 91.87 ± 0.374°
11	3.591	91.721	
12	3.609	91.127	

The Stokes parameters: S_0, S_1, S_2 and S_3 in Eq. (6) are functions of α, Φ and u. If α is known, Stokes parameters S_1, S_2 and S_3 can be measured by experiments. We can use Eq. (6) to solve twist angle Φ and, also, u that is a function of cell gap d and pretilt angle θ. From simulated results, we know that the occurrence of CM is insensitive to the change in pretilt angle so that we set the pretilt angle the same value as standard. Finally, we have derived the twist angles and cell gaps of the Mura sample at zero voltage from our experimental results as shown in Table 3.

3.2. Experiments to measure the Stokes parameters

The technique of measuring the Stokes parameters can be found in many optical textbooks [6]. Fig. 7 shows the experimental scheme to measure Stokes parameters. We set the incident light along z axis, and I_x, I_y and I_{45} are the intensities when the transmission axis of analyzer at 0°, 90° and 45° respectively. $I_{q,45}$ is the transmission intensity with quarter wave plate having a slow axis parallel to the y axis and the transmission axis of analyzer is set at 45°.

We obtain the Stokes parameters from the results of our measurements using following equations:

$$\begin{aligned} S_0 &= \frac{(I_x + I_y)}{(I_x + I_y)} = 1 \\ S_1 &= \frac{(I_x - I_y)}{(I_x + I_y)} \\ S_2 &= \frac{[2I_{45} - (I_x + I_y)]}{(I_x + I_y)} \\ S_3 &= \frac{[2I_{q,45} - (I_x + I_y)]}{(I_x + I_y)} \end{aligned} \tag{7}$$

Table 3 shows the derived Stokes parameters: S_1, S_2, S_3 for each point measured. Point number 1 – 6 are on the CM zone and point number 7 – 12 are on the Normal (non-Mura) zone.

4. Results and discussion

From our measured Stokes parameters (shown in Table 3) on six points of measurements at CM and Normal zones (shown in Fig. 2), respectively, we have derived the twist angles and cell gaps of the Mura sample at zero voltage using Eqs. (6) and (7) as shown in Table 4.

From the data of average cell gap and twist angle shown in the last column of Table 4, we calculate TR = 1.125 between CM and Normal zones, that is in a good agreement with TR = 1.13 obtained from direct measurements as described in Section 2. The good agreement leads to a conclusion that CM is caused mainly by stress-induced changes in the twist angle and cell gap of the TN medium within the Mura sample.

If we only consider the change in twist angle from 91.87° to 93.379° and neglect the change in the cell-gap, we obtain TR = 1.10. On the other hand, if we only consider the change of cell gap from 0.36 to 0.356 um and keep twist angle at 91.87°, we obtain TR = 1.0472. These results lead us to conclude that the change in TR (or occurrence of CM) is dominant by the stress-induced change in the twist angle and less sensitive to the induced change in cell gap of the Mura sample. Using the measured average twist angle and cell gap in the CM zone, we have calculated and obtained a maximum value of TR = 1.14 as the pretilt angle changed from 1 to 6°. The increase in TR is only about 1.3% from TR = 1.125 (at pretilt angle = 3.8°) so that the change in the pretilt angle can be neglected to cause the occurrences of CM.

After COG ACF process on TFT–TN panels, the CMs, if they occur, are caused mainly by the stress-induced change in the twist angle and cell gap of the in-panel LC medium. Here, we further consider how to optimize optical parameters of the TN cell to reduce the occurrence of CM after similar COG ACF process. According to reference [7], the light transmission, T, of a TN cell in a normally-black mode, is given by:

$$T = \frac{1}{2}\frac{\sin^2\left(\frac{\pi}{2}\sqrt{1+u^2}\right)}{1+u^2} \tag{8}$$

where u is a function of twist angle, cell gap, and pretilt angle of the TN medium, and is called the Mauguin parameter as specified by Eq. (4). According to Eq. (8), the variation in T is negligible for the first-order deviation of any parameter in twist angle, cell gap and pretilt angle away from u = 1.732 (the condition of Gooch–Tarry first minimum [7]). Therefore, to alleviate the occurrences of CM, the optimal design for the optical parameters of the TN cell is to satisfy the condition of Gooch–Tarry first minimum. In Fig. 8, we use Eq. (8) to plot transmission versus twist angle with cell gap as a parameter by assuming Δn = 0.1 and monochromatic light wavelength at 589 nm.

In Fig. 8, the cell gap of 5.1 μm satisfies the condition of Gooch–Tarry first minimum for a 90°-twist TN cell where u equals to 1.732 (the condition of Gooch–Tarry first minimum [7] where T in Eq. (8) is equal to minimum), and the light transmission of the cell between parallel polarizers is at minimum. It indicates that, when the cell gap is designed to satisfy the condition at the Gooch–Tarry first minimum, the transmission is very insensitive to the change of twist angle. Furthermore, Fig. 8 also shows that, at a twist angle near 90°, the change in transmission is less than 2% by varying the cell gap from 4.5 to 5.5 μm. Therefore, the results of Fig. 8 confirm

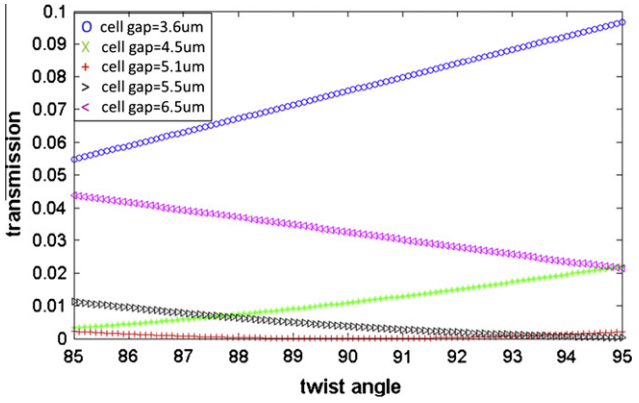

Fig. 8. Transmission vs. twist angle with cell gap as a parameter (Gooch–Tarry first minimum occurs at cell gap = 5.1 μm).

the conclusion that, by designing the optical parameters of the TN cell to satisfying the condition of Gooch–Terry first minimum, the probability for the occurrences of CM is much reduced on TFT–TN panels during and after COG ACF process. Such design is also suitable for the case of COG NCF (non-conductive film) process [8].

5. Conclusion

In this paper, we have utilized a transmission ratio (TR) as a key parameter to characterize the optical appearance of CM. First, we have used simulation to obtain the change in optical transmissions by varying optical parameters of cell gap, pretilt and twist angles of a TFT–TN panel from background values and concluded that TR was insensitive to the change in the pretilt angle of the Mura sample at zero voltage. We have set up an experimental scheme to measure TRs of the Mura sample at zero voltage directly, and obtained TR = 1.13. In order to calculate TRs on the Mura sample, we have set up another experimental scheme to measure the Stokes parameters of in-panel LC medium for points located within CM and Normal zones. We, then, have derived optical parameters of the Mura sample at zero voltage from measured Stokes parameters, and used them for the calculation of TR = 1.125. The good agreement between experimental and calculated results on TR leads to the conclusion that CM is caused mainly by stress-induced change in the twist angle and cell gap of the LC medium within the Mura sample. However, the calculated results on TRs using optical parameters of the Mura sample derived from the measured Stokes parameters seem to indicate that the occurrence of CM at zero voltage is dominant by the stress-induced change in the twist angle of the LC medium within the Mura sample but less sensitive and insensitive to the corresponding induced changes of the cell gap and the pretilt angle, respectively. By simulation, we also point out a way to reduce the occurrence of CM at zero voltage after COG ACF process by designing a cell gap for a 90°-twist TN panel to satisfy the condition of Gooch–Terry first minimum.

Acknowledgements

The authors acknowledge the financial support from National Science Council (NSC-99-2221-E-009-117), Dr. Jianmin Chen for providing the update version of simulation software LCDST, and Chimei Innolux Corporation for providing the 13.3-in. TFT–TN Mura sample for the measurements.

References

[1] Myung Jin Yim, Jinsang Hwang, Kyung Wook Paik, Anisotropic conductive films (ACFs) for ultra-fine pitch chip-on-glass (COG) applications, Int. J. Adhes. Adhes. 27 (2007) 77–84.
[2] Chin-Cheng Chang, Jihperng Leu, Effects of localized warpage and stress on chip-on-glass packaging induced light-leakage phenomenon in 13-in. TFT–LCD, in: SID2009 Int. Conf. Dig., 2009, pp. 838–842.
[3] Jianmin Chen, Liquid Crystal Display Simulation Tool, E-mail: benjaminxchen@yahoo.com.
[4] Z.H.O.U. Ying, H.E. Zhan, S.A.T.O. Susumu, A novel method for determining the cell thickness and twist angle of a twisted nematic cell by stokes parameter measurement, Jpn. J. Appl. Phys. 36 (1997) 2760–2764.
[5] Hiap Uew Ong, Origin and characteristics of the optical properties of general twisted nematic liquid-crystal displays, J. Appl. Phys. 64 (1988) 614.
[6] Deng-Ke Yang, Shin-Tson Wu, Fundamentals of Liquid Crystal Device, John Wiley & Sons, 2006 (Chapter 3).
[7] C.H. Gooch, H.A. Tarry, The optical properties of twisted nematic liquid crystal structures with twist angles ⩽ 90 degrees, J. Phys. D: Appl. Phys. 8 (1975) 1575.
[8] P.Y. Tang, W.-H. Sun, Kei-Hsiung Yang, A novel composite bump design for chip-on-glass package using non-conductive adhesive film, in: SID2009 Int. Symp. Dig. Tech. Papers, June 2009, pp. 834–837.